Refractory, Ceramic, and Composite Materials
Тугоплавкие, керамические и композиционные материалы

UDC 621-033.6 : 669.018.9; 621-033.6 : 666.1/.7; 621-033.6 : 666.1

https://doi.org/10.17073/1997-308X-2024-3-38-48

Research article
Научная статья

Self-propagating high-temperature synthesis and spark plasma sintering of high-entropy (Hf,Ta,Nb)(C,N) carbonitride

V. S. Suvorova, A. A. Nepapushev, D. S. Suvorov, K. V. Kuskov, D. O. Moskovskikh

National University of Science and Technology "MISIS"
4 Bld 1 Leninskiy Prosp., Moscow 119049, Russia

buynevich.vs@misis.ru

Abstract. In this research, we combined mechanical activation (MA), self-propagating high-temperature synthesis (SHS), and spark plasma sintering (SPS) methods to obtain a dense high-entropy (Hf,Ta,Nb)(C,N) carbonitride and studied its properties. To implement the SHS process, a mixture of initial metals and carbon was subjected to pre-treatment in a planetary mill in the low-energy mode, in which the jar rotation speed reached 350 rpm. We studied the evolution of microstructure and phase composition during the MA process. It has been established that after 60 min of treatment, Hf/Ta/Nb/C layered composite particles consisting of Hf, Ta, Nb and C submicron layers, with an average size of about 15 μm, were formed. However, according to the *X*-ray diffraction analysis, the components in the jar did not interact. SHS of Hf/Ta/Nb/C reactive mixtures was performed in a nitrogen atmosphere (P = 0.8 MPa); after synthesis, two isomorphic (Hf,Ta,Nb)(C,N) phases of the *Fm*-3*m* (225) space group with lattice parameters of a = 0.4476 nm (71 wt. %) and a = 0.4469 nm (22 wt. %) were revealed in the powder. After SHS, the average size of agglomerates was 10 μm and their morphology resembled that of composite particles after MA. The agglomerates formed during SHS consisted of pores and round-shaped particles ranging in size from 0.5 to 2 μm, which was caused by the melting of metal components in the combustion zone and rapid crystallization of product grains from the melt, followed by subsequent recrystallization. Spark plasma sintering at a temperature of 2000 °C, a pressure of 50 MPa and a holding time of 20 min enabled to obtain a single-phase high-entropy $(Hf_{0.33}Ta_{0.33}Nb_{0.33})C_{0.5}N_{0.3}$ material with a lattice parameter of 0.4482 nm characterized by a high relative density of 98 %, a hardness of 21.5 ± 0.4 GPa, a Young's modulus of 458 ± 10 GPa, and a fracture toughness value of 3.7 ± 0.3 MPa·m$^{1/2}$.

Keywords: high-entropy ceramics, high-entropy carbonitride, mechanical activation, self-propagating high-temperature synthesis, ceramics, spark plasma sintering

Acknowledgements: This work was supported by the Russian Science Foundation grant No. 19-79-10280П.

For citation: Suvorova V.S., Nepapushev A.A., Suvorov D.S., Kuskov K.V., Moskovskikh D.O. Self-propagating high-temperature synthesis and spark plasma sintering of high-entropy (Hf,Ta,Nb)(C,N) carbonitride. *Powder Metallurgy and Functional Coatings*. 2024;18(3):38–48. https://doi.org/10.17073/1997-308X-2024-3-38-48

Самораспространяющийся высокотемпературный синтез и искровое плазменное спекание высокоэнтропийного карбонитрида (Hf,Ta,Nb)(C,N)

В. С. Суворова, А. А. Непапушев, Д. С. Суворов, К. В. Кусков, Д. О. Московских

Национальный исследовательский технологический университет «МИСИС»
Россия, 119049, г. Москва, Ленинский пр-т, 4, стр. 1

buynevich.vs@misis.ru

Аннотация. В работе комбинацией методов механического активирования (МА), самораспространяющегося высокотемпературного синтеза (СВС) и искрового плазменного спекания (ИПС) получен плотный высокоэнтропийный карбонитрид (Hf,Ta,Nb)(C,N) и исследованы его свойства. Для реализации процесса СВС смесь исходных металлов с углеродом подвергали предварительной обработке в планетарной мельнице в низкоэнергетическом режиме, при котором скорость вращения барабанов составляла 350 об/мин. Была исследована эволюция микроструктуры и фазового состава в процессе МА. Установлено, что после обработки в течение 60 мин происходит формирование слоистых композиционных частиц Hf/Ta/Nb/C, имеющих средний размер порядка 15 мкм и состоящих из субмикронных слоев Hf, Ta, Nb и C. При этом, согласно данным рентгенофазового анализа, взаимодействия компонентов в барабане не происходило. СВС реакционных смесей Hf/Ta/Nb/C проводили в атмосфере азота (P = 0,8 МПа), после синтеза в порошке были обнаружены две изоморфные фазы (Hf,Ta,Nb)(C,N) пространственной группы $Fm\text{-}3m$ (225) с различными параметрами решетки: a = 0,4476 нм (71 мас. %) и a = 0,4469 нм (22 мас. %). Морфология частиц после СВС повторяла морфологию композиционных частиц после МА, средний размер агломератов составлял 10 мкм. Сформировавшиеся в процессе СВС агломераты состояли из частиц округлой формы размером от 0,5 до 2 мкм и пор, что обусловлено плавлением металлических компонентов в зоне горения, быстрой кристаллизацией зерен продукта из расплава и их последующей рекристаллизацией. Процесс ИПС при температуре 2000 °C, давлении прессования 50 МПа и времени выдержки 20 мин позволил получить однофазный высокоэнтропийный материал $(Hf_{0,33}Ta_{0,33}Nb_{0,33})C_{0,5}N_{0,3}$ с параметром решетки 0,4482 нм, который характеризовался высокой относительной плотностью 98 %, твердостью 21,5 ± 0,4 ГПа, модулем Юнга 458 ± 10 ГПа и значением трещиностойкости 3,7 ± 0,3 МПа·м$^{1/2}$.

Ключевые слова: высокоэнтропийная керамика, высокоэнтропийный карбонитрид, механическое активирование, самораспространяющийся высокотемпературный синтез, керамика, искровое плазменное спекание

Благодарности: Работа выполнена при финансовой поддержке гранта РНФ № 19-79-10280П.

Для цитирования: Суворова В.С., Непапушев А.А., Суворов Д.С., Кусков К.В., Московских Д.О. Самораспространяющийся высокотемпературный синтез и искровое плазменное спекание высокоэнтропийного карбонитрида (Hf,Ta,Nb)(C,N). *Известия вузов. Порошковая металлургия и функциональные покрытия*. 2024;18(3):38–48.
https://doi.org/10.17073/1997-308X-2024-3-38-48

Introduction

The development of pioneer industries poses a challenge for researchers to find new materials with high mechanical properties that can withstand high temperatures. In recent years, scientists have focused on high-entropy ceramics (HECs) with a configurational entropy of mixing $S_{mix} \geq 1/.61R$ [1]. Unlike high-entropy alloys [2], HECs contain cations or anions sublattices [3], which gives this class of materials a wide structural diversity and controllable properties.

Among HECs, the compounds based on transition metals, IVB (Ti, Zr, Hf) and VB (V, Nb, Ta) groups of the periodic table, which have higher properties in comparison, for example, with binary carbides and nitrides, are most suitable for high-temperature applications. For example, the authors of [4] used spark plasma sintering (SPS) of a mixture of TaC, ZrC and NbC powders to synthesize single-phase (Ta,Zr,Nb)C carbide with high flexural strength at elevated temperatures (1600–2000 °C). In [5], high-entropy (HfTaZrTi)C and (HfTaZrNb)C carbides revealed a significantly enhanced hardness (36.1 ± 1.6 GPa) compared to HfC (31.5 ± 1.3 GPa) and (Hf,Ta)C (32.9 ± 1.8 GPa).

High-entropy carbonitride ceramics is also of importance for fundamental research and practical applications. A number of studies have shown that carbide sublattice nitrogen doping contributes to improving properties, including mechanical ones, as strong *Me*–(C,N) covalent bonds and the C≡N triple bond [6–8] are formed. The study [9] demonstrated

that the introduction of an additional metal component into the initial Ti–Zr–Hf–C–N system helps to increase the configuration entropy and, as a consequence, to enhance mechanical properties. As a result, extremely high fracture toughness (8.4 MPa·m$^{1/2}$) was reached in a five-component carbonitride $(Ti_{0.2}Zr_{0.2}Hf_{0.2}Nb_{0.2}Ta_{0.2})(C_{0.5}N_{0.5})$.

Previously, the authors of this paper obtained a double carbonitride in the Ta–Hf–C–N system, which demonstrated excellent mechanical properties and oxidation resistance [10; 11]. The introduction of an additional metal component Nb in the equiatomic ratio is expected to improve the mechanical properties of tantalum-hafnium carbonitride $(Ta_{0.5}Hf_{0.5})(C,N)$.

Dense high-entropy carbonitrides are commonly prepared by sintering a mixture of transition metal carbides and nitrides [12–14]. However, this method requires elevated temperatures and long exposures to complete the diffusion processes. The self-propagating high-temperature synthesis (SHS) method enables to significantly reduce the time for obtaining powder of complex multicomponent compounds. The subsequent spark plasma sintering pushes down energy costs for the fabrication of dense ceramics.

In this regard, the objective of this study was to obtain high-density (Hf,Ta,Nb)(C,N) carbonitride by combining the methods of mechanical activation (MA), self-propagating high-temperature synthesis and spark plasma sintering, and to investigate the mechanical properties of the resulting material.

Materials and methods

The precursors were hafnium powders GFM-1 (98.8 %, ≤ 180 μm), tantalum TaP-1 (99.9 %, from 40 to 60 μm), niobium NbP-1a (99.9 %, from 40 to 63 μm) and carbon black P804T(99.5 %, ≤ 0.2 μm). Before SHS, the Hf + Ta + Nb + C powder mixture was subjected to MA in a high-energy planetary ball mill "Activator-2S" (CJSC Activator, Russia) in an atmosphere of high purity argon (99.998 %): the ratio of the balls to powder mass was 20:1 (360 g : 18 g), gas pressure inside the cylinders stood at 0.6 MPa, and rotation speed was 350 rpm. To study the evolution of the phase composition and microstructure, the powder was removed from the jar after MA conducted for 5, 30, 45 and 60 min.

SHS was performed in the constant pressure reactor in a nitrogen atmosphere (grade *1*, 99.999 %). The reactor chamber was pre-evacuated, then nitrogen was pumped until *P* reached 0.8 MPa. The self-sustaining exothermic reaction was initiated by briefly applying voltage to the tungsten coil connected to the power source.

SHS powders were consolidated by spark plasma sintering using a Labox 650 unit (SinterLand, Japan) in an argon atmosphere at a temperature of 2000 °C, press pressure of 50 MPa, and a holding time of 20 min. The temperature was raised to the given value at a rate of 100 °C/min.

The samples microstructure, as well as their elemental composition, was studied using a JEOL JSM7600F scanning electron microscope (SEM) (JEOL Ltd., Japan) equipped with an X-MAX 80 mm^2 *X*-ray microanalysis system (Oxford Instruments, UK), at an accelerating voltage of 15 kV. The sizes of particles after MA and SHS were analyzed on a Bettersizer ST analyzer (Bettersize Instruments LTD, China) with wet dispersion.

The phase composition was studied using the *X*-ray diffraction analysis (XRD) on a Dron-4-07 diffractometer (JSC Research Center Burevestnik, Russia) with CuK_α radiation in the step scanning mode (scanning step 0.1°), the angles ranging from 20 to 80° with 2 s exposure. The ICDD PDF databases were used to analyze the resulting spectra. The Rietveld method was applied to calculate the lattice parameters and to conduct the quantitative phase analysis.

A TC-600 (Leco, USA) instrument estimated the amount of nitrogen and oxygen in the compounds by IR adsorption (for oxygen) and thermal conductivity (for nitrogen) analysis during the reduction melting of the samples in a resistance furnace in a helium flow. A CS-600 (Leco) instrument was used to measure the carbon content. For this purpose, the samples were subjected to oxidative melting in an induction furnace and the amount of CO_2 released was measured by IR absorption. The mass content of iron was determined by atomic emission spectral analysis on an iCAP 6000 echelle spectrometer (Thermo Fisher, USA).

The configurational entropy of mixing S_{mix} of a covalently bound compound was calculated using the formula [15]:

$$S_{mix} = -R\left[\left(\sum_{i=1}^{N} x_i \ln x_i\right)_{cationic} + \left(\sum_{j=1}^{N} x_j \ln x_j\right)_{anionic}\right],$$

where R is the universal gas constant, x_i and x_j are the mole fractions of cationic and anionic elements, respectively.

The relative density of samples after SPS was calculated as the ratio of hydrostatic to pycnometric density. The hydrostatic density of the samples was determined by hydrostatic weighing under GOST 20018-74 [16]. Pycnometric density was mea-

sured using a Ultrapycnometer 1000 helium pycnometer (Quantachrome Instruments, USA).

A Micro-Hardness Tester (CSM Instruments, Switzerland) was used to measure Young's modulus (E) at a 100 mN applied load.

We used a Durascan 70 hardness testing machine (Struers ApS, Denmark) to estimate hardness (HV) by the Vickers method, GOST 2999-75 [17]. A load of 30 N was applied for 10 s. At least 10 measurements were taken with each sample. We used the Anstis equation to assess the fracture toughness (K_{1c}) [18].

Results and discussion

Before conducting SHS, the powder mixture consisting of Hf, Ta, Nb and C was subjected to mechanical activation to enhance its reactivity by reducing the particle size, accumulating defects and forming layered composite particles throughout the entire volume of the powder. The large contact area between the components of the mixture in composite particles facilitates and significantly accelerates the diffusion interaction between them during the SHS process [19].

Fig. 1 shows X-ray diffraction patterns of the Hf + + Ta + Nb + C reaction mixture after mechanical activations (MA) of different durations in a planetary ball mill. After the 5 min MA, the X-ray diffraction pattern features peaks of individual elements: Nb and Ta of Im-3m (229) space group, as well as hexagonal Hf ($P6_3/mmc$ (194)). Peaks of carbon black (C) are not identified due to its X-ray amorphism.

As the MA duration increases, the peaks widen and their intensity significantly decreases as the components crystal lattices deform during mechanical processing. After the 60 min MA, the phase composition remains unchanged, the X-ray diffraction pattern still shows diffraction peaks of the mixture metal components, while the reaction products, which lead to a drop in the accumulated energy and, consequently, reduced reactivity of the mixture, are not formed.

The evolution of the structure of the Hf + Ta + + Nb + C reaction mixture during MA was studied using scanning electron microscopy (SEM) and X-ray microanalysis (XRMA) (Fig. 2). The non-activated powder mixture mostly consists of polygonal Hf, Ta and Nb particles ranging in size from 10 to 160 μm, as well as carbon black C agglomerates (Fig. 2, *a*). At the start of mechanical activation in the low-energy mode (from 0 to 30 min, Fig. 2, *b*, *c*), the mixture particles are crushed and flattened, new surfaces without oxide films or other impurities are formed, the contact area between Hf, Ta, Nb and C increases. The flattened particles interact with each other with their atomically pure surfaces; as a result, after τ_{MA} = 30 min, the first layered composite particles are formed (Fig. 2, *c*). With longer mechanical activation (Fig. 2, *d*, *e*), the content of particles of initial components in the reaction mixture drops, the composite particles crush into smaller ones and the thickness of the Hf, Ta, Nb and C layers decreases. After τ_{MA} = 60 min (Fig. 2, *e*), the Hf/Ta/Nb/C layered composite particles are formed throughout the entire volume of the reaction mixture. The size of composite particles varies from 1 to 40 μm, the average size is 13 μm. Although mechanical activation was carried out in steel jars with steel grinding balls for 60 min, the content of iron and chromium does not exceed 0.5 and 0.05 wt. %, respectively, which is attributed to the use of low-energy mode (350 rpm) and the presence of a "lubricant" in the form of carbon black, which prevents grinding [20].

Thus, mechanical activation for 60 min in the low-energy mode contributes to the formation of Hf/Ta/Nb/C layered composite particles throughout the entire volume of the powder, however, reaction products inside the jars, which reduce the mixture reactivity, are not formed.

Fig. 3 shows an X-ray diffraction pattern of the powder after treatment in the mill for 60 min and subsequent

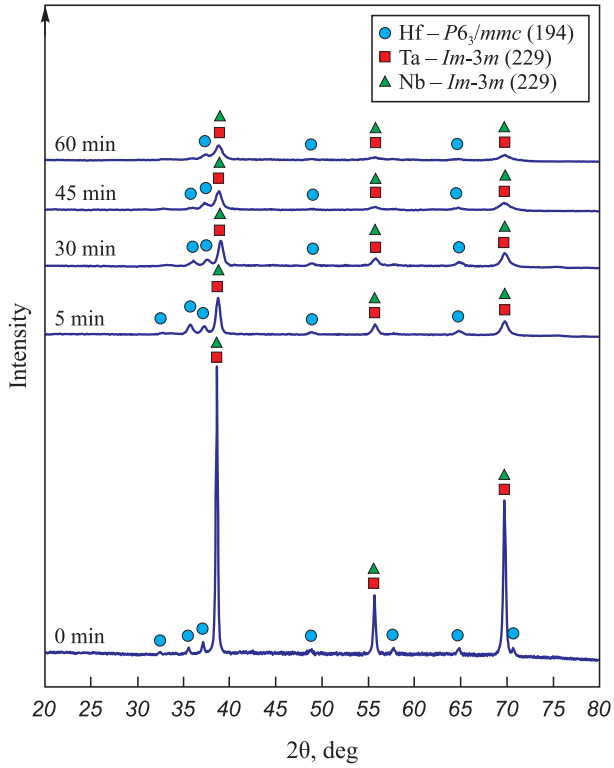

Fig. 1. The X-ray diffraction patterns of the Hf + Ta + Nb + C reactive mixture after MA of different durations

Рис. 1. Дифрактограммы реакционной смеси Hf + Ta + Nb + C после различного времени МА

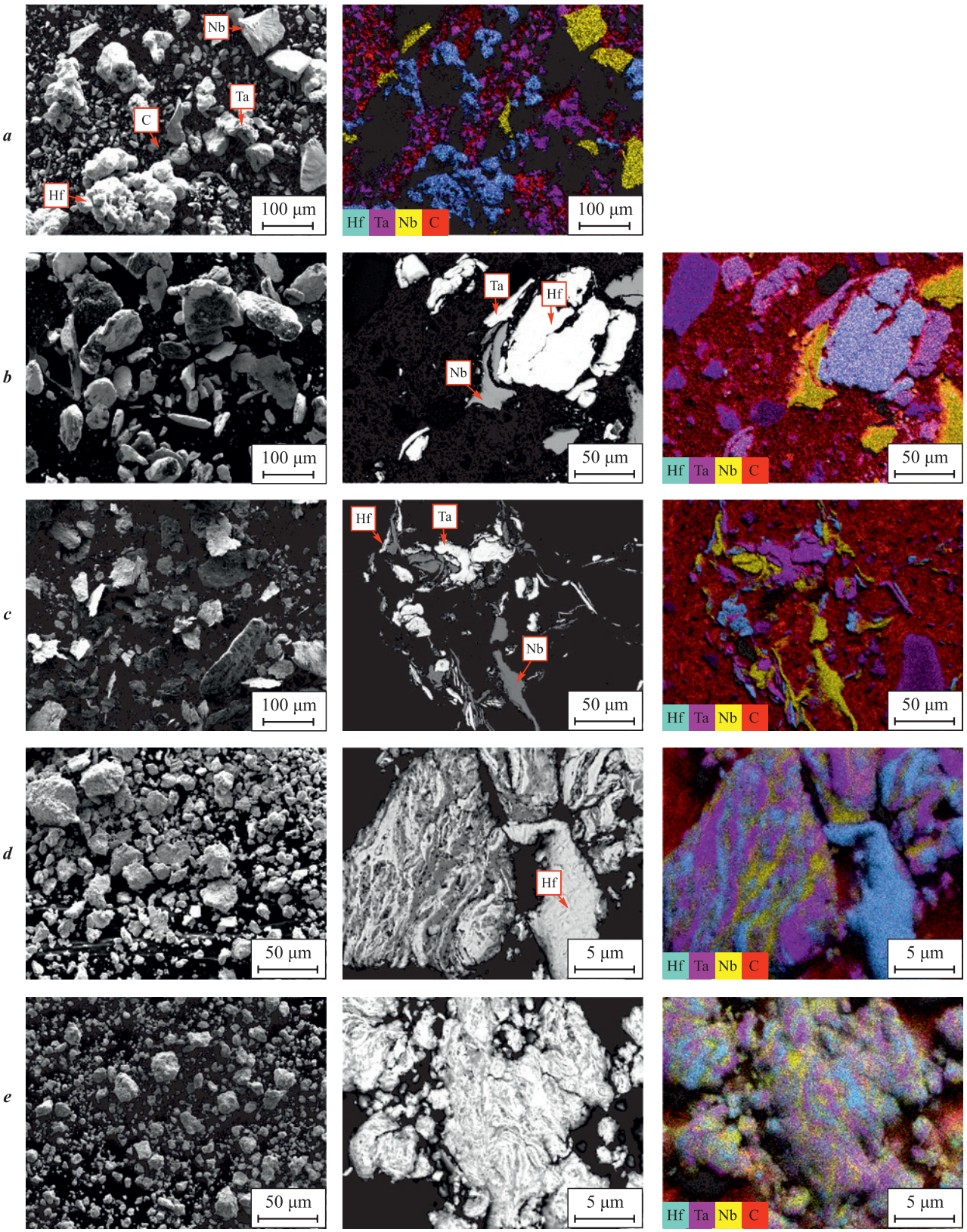

Fig. 2. The morphology, cross-section microstructures and element distribution maps of the Hf + Ta + Nb + C reactive mixture after MA of different durations

τ_{MA}, min: ***a*** – 0, ***b*** – 5, ***c*** – 30, ***d*** – 45, ***e*** – 60

Рис. 2. Морфология, микроструктуры поперечных сечений и карты распределения элементов реакционной смеси Hf + Ta + Nb + C после различного времени МА

τ_{MA}, мин: ***a*** – 0, ***b*** – 5, ***c*** – 30, ***d*** – 45, ***e*** – 60

SHS in a nitrogen atmosphere (P = 0.8 MPa). We can see that after synthesis, the phase composition fundamentally changes compared to the powder after MA; the X-ray diffraction pattern features widened and asymmetric peaks due to the formation of two isomorphic phases (Hf,Ta,Nb)(C,N) of the Fm-3m (225) space group with different lattice parameters – 0.4476 nm (71 wt. %) and 0.4469 nm (22 wt. %).

During filtration combustion of layered composite particles in nitrogen, the first step involves the formation of the nonstoichiometric carbide [19], which propagates at a very high speed, therefore, interaction with nitrogen occurs in the aftercombustion zone only [21]. High cooling rates lead to uneven nitriding throughout the sample volume, resulting in the formation of phases with different N contents [26]. The X-ray diffraction pattern also reveals low-intensity peaks of orthorhombic and monoclinic HfO_2 – based on the calculations by the Rietveld method, their content in the powder after SHS is 4 and 3 wt. %, respectively.

After SHS, the morphology of the product agglomerates (Fig. 4, *a*) predictably repeats the morphology of the composite particles after MA (Fig. 2, *e*), the average size of the agglomerates being ~30 μm. The extensive contact surfaces between the reagents in layered composite particles contributed to a significant acceleration of the diffusion interaction between them during the combustion process, as a result the morphology of the particles remained practically unchanged [22; 23].

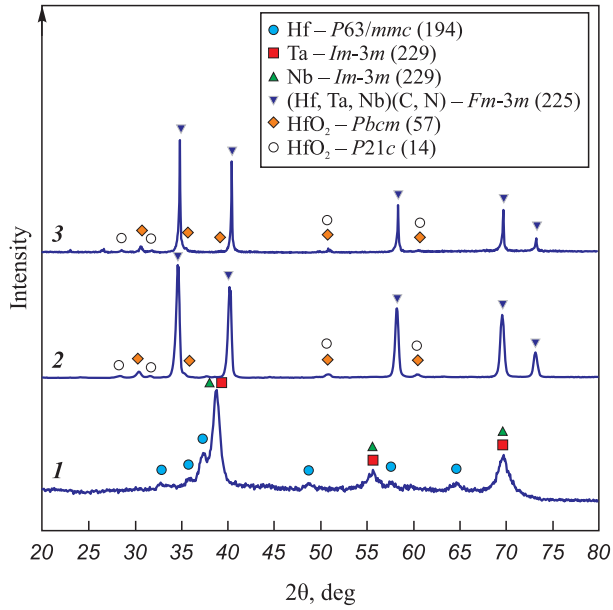

Fig. 3. *X*-ray diffraction patterns of the reaction mixture after 60 min MA (***1***), (Hf,Ta,Nb)(C,N) after SHS (***2***) and SPS (***3***)

Рис. 3. Дифрактограммы реакционной смеси после МА в течение 60 мин (***1***), (Hf,Ta,Nb)(C,N) после СВС (***2***) и ИПС (***3***)

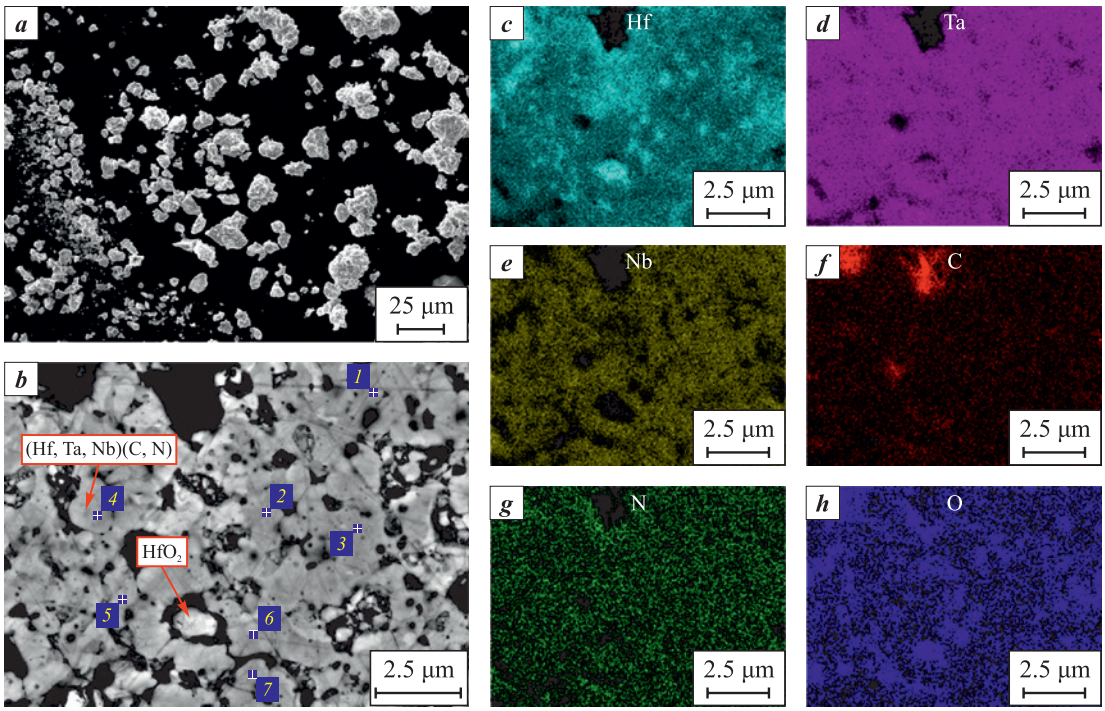

Fig. 4. Morphology of the (Hf,Ta,Nb)(C,N) agglomerates after SHS (***a***), cross-section microstructure (***b***), maps of the elements distribution in the agglomerate (***c***–***h***)

Рис. 4. Морфология агломератов (Hf,Ta,Nb)(C,N) после СВС (***a***), микроструктура поперечного сечения (***b***), карты распределения элементов в агломерате (***c***–***h***)

Table 1. **X-ray microanalysis of the (Hf,Ta,Nb)(C,N) cross-section after SHS (at. %)**

Таблица 1. **Микрорентгеноспектральный анализ поперечного сечения (Hf,Ta,Nb)(C,N) после СВС (ат. %)**

Spectrum number	Hf	Ta	Nb	C	N	O	Σ
1	14.8	14.3	14.3	40.2	12.9	3.5	100.0
2	13.1	13.9	13.5	52.5	1.9	5.1	100.0
3	14.8	14.4	15.1	47.9	3.2	4.6	100.0
4	13.7	14.9	14.6	48.9	4.1	3.8	100.0
5	13.7	13.8	13.9	48.3	4.6	5.7	100.0
6	12.5	12.9	13.1	51.8	5.2	4.5	100.0
7	14.8	14.5	14.9	43.7	6.9	5.2	100.0

When examining the cross section of the agglomerate (Fig. 4, *b*), we can see pores and rounded particles ranging in size from 0.5 to 2 μm. According to EDS (Fig. 4, *c*–*g*, Table 1), in the product (Hf,Ta,Nb)(C,N) (gray areas), the elements Hf, Ta, Nb and C are uniformly distributed, the nitrogen content in the particles fluctuating from 2 to 13 at. %. In addition to the main phase, HfO_2 inclusions (light gray areas in Fig. 4, *b*, *c*, *h*) are observed in the agglomerates.

As with the Hf–C–N [24], Ta–Hf–C–N [11] and Hf–Zr–C–N systems, the rounded particles are formed [25; 26] due to melting of the mixture metal components in the reaction zone, rapid crystallization of product grains from the melt and their subsequent recrystallization [27; 28]. The agglomerates structure after SHS is porous as gas releases during the combustion process.

Spark plasma sintering was performed in the mode previously tested on the Ta–Hf–C–N system [10; 11]. The *X*-ray diffraction pattern of sintered (Hf,Ta,Nb)(C,N) carbonitride is shown in Fig. 3. When exposed to high temperature, the carbonitride peaks became narrower and more symmetrical, suggesting homogenization of the chemical composition, ordering of the crystal structure and an increased size of crystallites after sintering; the lattice parameter value after SPS was 0.4482 nm. Compared to the powder after SHS, the content of orthorhombic and monoclinic HfO_2 increased to 7 and 5 wt. %.

A typical microstructure of (Hf,Ta,Nb)(C,N) carbonitride after SPS, as well as an elements distribution map are shown in Fig. 5. The particle size of the main phase (Hf,Ta,Nb)(C,N) (gray areas) varies from 2 to 15 μm. According to EDS (Fig. 5, *b*–*f*), the elements Hf, Ta, Nb, C and N are uniformly distributed. However, the structure of the bulk material features HfO_2 inclusions (light areas, Fig. 5, *a*, *b*, *g*) along the boundaries of the main phase, which confirms the *X*-ray diffraction data. The pycnometric density of the bulk carbonitride amounted to 11.06 ± 0.05 g/cm^3, the hydrostatic density was 10.8 ± 0.2 g/cm^3, which, in turn, corresponds to 98 % of the relative density and is consistent with the microstructural analysis data.

Based on the results of chemical analysis, it can be concluded that the carbon content in the (Hf,Ta,Nb)(C,N)

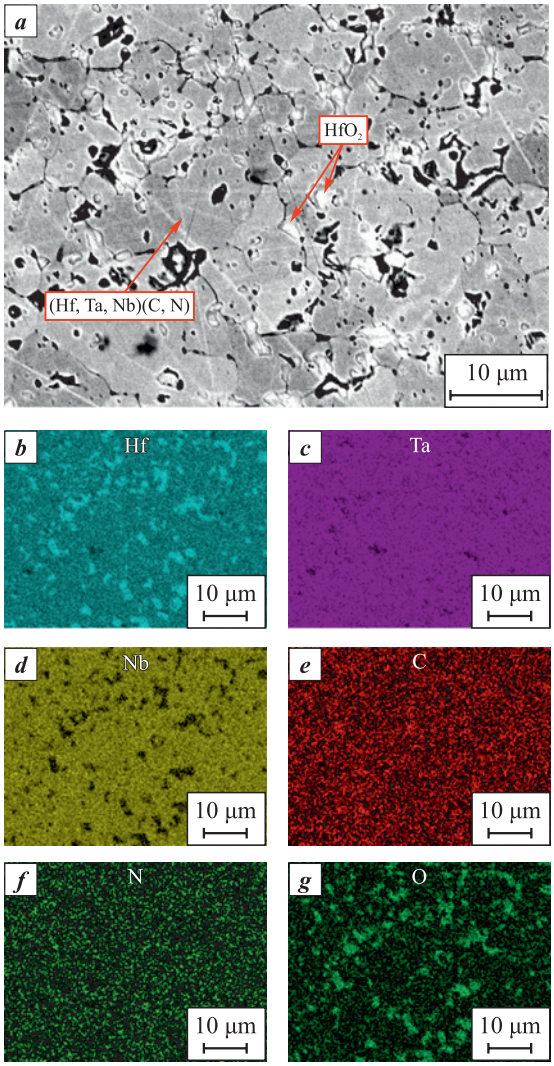

Fig. 5. (Hf,Ta,Nb)(C,N) microstructure (***a***) and elements distribution map after SPS (***b***–***g***)

Рис. 5. Микроструктура (Hf,Ta,Nb)(C,N) (***a***) и карты распределения элементов после ИПС (***b***–***g***)

Table 2. **The mechanical properties of high-entropy (Hf,Ta,Nb)(C,N) carbonitride and similar materials**

Таблица 2. **Механические свойства высокоэнтропийного карбонитрида (Hf,Ta,Nb)(C,N) и аналогичных материалов**

Sample	ρ, %	*HV*, GPa	*E*, GPa	K_{1c}, MPa·m$^{1/2}$
(Hf,Ta,Nb)(C,N)	98.0 ± 0.5	21.5 ± 0.4	458 ± 10	3.7 ± 0.3
$(Ta_{0.5}Hf_{0.5})C_{0.51}N_{0.4}$ [11]	98.0	18.7 ± 0.1	516	–
$(Ti,V,Nb,Ta)(C_{0.7}N_{0.3})$ [31]	95.6	19.1	437.5	2.0
$(Hf_{0.2}Zr_{0.2}Ta_{0.2}Nb_{0.2}Ti_{0.2})(N_{0.5}C_{0.5})$ [32]	95.9	19.5 ± 0.3	429 ± 10	2.8 ± 0.3
$(Ti_{0.33}Zr_{0.33}Hf_{0.33})(C_{0.5}N_{0.5})$ [9]	–	~16.0	~460	5.7
$(Ti_{0.25}Zr_{0.25}Hf_{0.25}Nb_{0.25})(C_{0.5}N_{0.5})$ [9]	–	~18.0	~450 ± 140	6.9
$(Ti_{0.2}Zr_{0.2}Hf_{0.2}Nb_{0.2}Ta_{0.2})(C_{0.5}N_{0.5})$ [9]	–	~21.0	~460	8.4
(NbTaZr)C [33]	99.5	20.24 ± 0.87	505	3.07
$(Zr_{0.25}Nb_{0.25}Ti_{0.25}V_{0.25})C$ [34]	95.1	19.1 ± 0.5	460.4 ± 19.3	4.7 ± 0.5
$(Hf_{0.2}Zr_{0.2}Ta_{0.2}Nb_{0.2}Ti_{0.2})C$ [35]	93.0	15.0	479	–

sample corresponds to the amount of carbon in the initial reaction mixture and amounts to 3.8 ± 0.2 wt. %, while nitrogen and oxygen content are 2.3 ± 0.1 and 0.8 ± 0.2 wt. %, respectively. The chemical formula of bulk carbonitride can be written as follows: $(Hf_{0.33}Ta_{0.33}Nb_{0.33})C_{0.5}N_{0.3}$. For the resulting compound, the configuration entropy of mixing (S_{mix}) was 1.8, which meets the criteria for high-entropy materials $S_{mix} \geq 1.61R$ [29; 30].

Microhardness, Young's modulus and fracture toughness were studied on sintered samples. The mechanical properties of high-entropy (Hf,Ta,Nb)(C,N) carbonitride and similar materials are presented in Table 2. High-entropy (Hf,Ta,Nb)(C,N) carbonitride is characterized by higher hardness compared to $(Ta_{0.5}Hf_{0.5})C_{0.51}N_{0.4}$ tantalum-hafnium carbonitride obtained in a similar way [11]. Considering that (Hf,Ta,Nb)(C,N) and $(Ta_{0.5}Hf_{0.5})C_{0.51}N_{0.4}$ have almost the same grain size (2–15 μm and 6–10 μm, respectively), it can be assumed that the introduction of Nb into the composition of $(Ta_{0.5}Hf_{0.5})C_{0.51}N_{0.4}$ tantalum-hafnium carbonitride contributed to increased hardness caused by enhanced configurational entropy of mixing. The similar effect was demonstrated in [9], where the hardness and fracture toughness increase with enhancing configurational entropy of mixing. Compared to other multicomponent carbonitrides [9; 31; 32] and carbides [33–35], (Hf,Ta,Nb)(C,N) demonstrated higher hardness (21.5 ± 0.4 GPa), as well as a comparable value of fracture toughness (3.7 ± 0.3 MPa ·m$^{1/2}$).

Conclusions

1. We studied the impact of MA duration on the structure and phase composition of the Hf + Ta + Nb + C reaction mixture. It has been demonstrated that mechanical treatment in the low-energy mode for 60 min contributes to the formation of layered composite particles with an average size of 13 μm throughout the entire powder volume.

2. The powder after SHS included two isomorphic phases (Hf,Ta,Nb)(C,N) with lattice parameters of 0.4476 nm and 0.4469 nm *Fm*-3*m* (225) space group.

3. A dense high-entropy $(Hf_{0.33}Ta_{0.33}Nb_{0.33})C_{0.5}N_{0.3}$ carbonitride with a relative density of 98 %, hardness of 21.5 ± 0.4 GPa, Young's modulus of 458 ± 10 GPa and fracture toughness of 3.7 ± 0.3 MPa·m$^{1/2}$ was fabricated from the synthesized powder using the spark plasma sintering method.

References / Список литературы

1. Xiang H., Xing Y., Dai F.Z., Wang H., Su L., Miao L., Zhang G., Wang Y., Qi X., Yao L., Wang H., Zhao B., Li J., Zhou Y. High-entropy ceramics: Present status, challenges, and a look forward. *Journal of Advanced Ceramics*. 2021;10(3):385–441. https://doi.org/10.1007/s40145-021-0477-y
2. Dewangan S.K., Mangish A., Kumar S., Sharma A., Ahn B., Kumar V. A review on high-temperature applicability: A milestone for high entropy alloys. *Engineering Science and Technology, an International Journal*. 2022;35:101211. https://doi.org/10.1016/j.jestch.2022.101211
3. Akrami S., Edalati P., Fuji M., Edalati K. High-entropy ceramics: Review of principles, production and applications. *Materials Science and Engineering: R: Reports*. 2021;146:100644. https://doi.org/10.1016/j.mser.2021.100644
4. Demirskyi D., Borodianska H., Suzuki T.S., Sakka Y., Yoshimi K., Vasylkiv O. High-temperature flexural strength performance of ternary high-entropy carbide consolidated via spark plasma sintering of TaC, ZrC and NbC. *Scripta Materialia*. 2019;164:12–16. https://doi.org/10.1016/j.scriptamat.2019.01.024

5. Castle E., Csanádi T., Grasso S., Dusza J., Reece M. Processing and properties of high-entropy ultra-high temperature carbides. *Scientific Reports*. 2018;8:8609. https://doi.org/10.1038/s41598-018-26827-1

6. Hong Q.J., Van De Walle A. Prediction of the material with highest known melting point from ab initio molecular dynamics calculations. *Physical Review B*. 2015;92(2): 020104. https://doi.org/10.1103/PhysRevB.92.020104

7. Zhang X., Li X., Zuo J., Luo R., Wang J., Qian Y., Li M., Xu J. Characterization of thermophysical and mechanical properties of hafnium carbonitride fabricated by hot pressing sintering. *Journal of Materials Research and Technology*. 2023;23:4432–4443. https://doi.org/10.1016/j.jmrt.2023.02.099

8. Peng Z., Sun W., Xiong X., Xu Y., Zhou Z., Zhan Z., Zhang H., Zeng Y. Novel nitrogen-doped hafnium carbides for advanced ablation resistance up to 3273 K. *Corrosion Science*. 2021;189:109623. https://doi.org/10.1016/j.corsci.2021.109623

9. Zhang P., Liu X., Cai A., Du Q., Yuan X., Wang H., Wu Y., Jiang S., Lu Z. High-entropy carbide-nitrides with enhanced toughness and sinterability. *Science China Materials*. 2021;64(8):2037–2044. https://doi.org/10.1007/s40843-020-1610-9

10. Suvorova V.S., Nepapushev A.A., Moskovskikh D.O., Kuskov K.V. Fabrication and oxidation resistance of the non-stoichiometric tantalum-hafnium carbonitride. *Powder Metallurgy and Functional Coatings*. 2022;(3):45–54. https://doi.org/10.17073/1997-308X-2022-3-45-54

Суворова В.С., Непапушев А.А., Московских Д.О., Кусков К.В. Получение нестехиометрического танталгафниевого карбонитрида и исследование его окислительной стойкости. *Известия вузов. Порошковая металлургия и функциональные покрытия*. 2022;(3):45–54. https://doi.org/10.17073/1997-308X-2022-3-45-54

11. Buinevich V.S., Nepapushev A.A., Moskovskikh D.O., Kuskov K.V., Yudin S.N., Mukasyan A.S. Ultra-high-temperature tantalum-hafnium carbonitride ceramics fabricated by combustion synthesis and spark plasma sintering. *Ceramics International*. 2021;47(21):30043–30050. https://doi.org/10.1016/j.ceramint.2021.07.180

12. Dippo O.F., Mesgarzadeh N., Harrington T.J., Schrader G.D., Vecchio K.S. Bulk high-entropy nitrides and carbonitrides. *Scientific Reports*. 2020;10(1):21288. https://doi.org/10.1038/s41598-020-78175-8

13. Wang Y., Csanádi T., Zhang H., Dusza J., Reece M.J. Synthesis, microstructure, and mechanical properties of novel high entropy carbonitrides. *Acta Materialia*. 2022;231:117887. https://doi.org/10.1016/j.actamat.2022.117887

14. Peng Z., Sun W., Xiong X., Zhang H., Guo F., Li J. Novel refractory high-entropy ceramics: Transition metal carbonitrides with superior ablation resistance. *Corrosion Science*. 2021;184:109359. https://doi.org/10.1016/j.corsci.2021.109359

15. Peng C., Tang H., He Y., Lu X., Jia P., Liu G., Zhao Y., Wang M. A novel non-stoichiometric medium-entropy carbide stabilized by anion vacancies. *Journal of Materials Science & Technology*. 2020;51:161–166. https://doi.org/10.1016/j.jmst.2020.02.049

16. GOST 20018-74 (ST SEV 1253-78, ISO 3369-75). Sintered hard alloys: Density determination method (with changes No. 1, 2, 3). Moscow: Gosstandart SSSR, 1991. 11 p. (In Russ.).

ГОСТ 20018-74 (СТ СЭВ 1253-78, ИСО 3369-75). Сплавы твердые спеченные: Метод определения плотности (с изменениями № 1, 2, 3). М.: Госстандарт СССР, 1991. 11 с.

17. GOST 2999-75. Metals and alloys: Vickers hardness measurement method (with changes No. 1, 2). Moscow: Management of standardization and certification of raw materials and materials, 1986. (In Russ.).

ГОСТ 2999-75. Металлы и сплавы: Метод измерения твердости по Виккерсу (переизд. с изм. 1, 2). М.: Управление стандартизации и сертификации сырья и материалов, 1986.

18. Anstis G.R., Chantikul P., Lawn B.R., Marshall D.B. A critical evaluation of indentation techniques for measuring fracture toughness: I, direct crack measurements. *Journal of the American Ceramic Society*. 1981;64(9):533–538. https://doi.org/10.1111/j.1151-2916.1981.tb10320.x

19. Suvorova V.S. Fabrication of ultra-high-temperature ceramics based on hafnium carbonitride by self-propagating high-temperature synthesis: Diss. Cand. Sci. (Eng.). Moscow: MISIS, 2022. (In Russ.).

Суворова В.С. Получение тугоплавких керамик на основе карбонитрида гафния методом самораспространяющегося высокотемпературного синтеза: Дис. … канд. техн. наук. М.: МИСИС, 2022.

20. Liu G., Li J., Chen K. Combustion synthesis: Handbook of combustion: Online: Wiley-VCH Verlag GmbH&Co, 2015. 62 p. https://doi.org/10.1002/9783527628148.hoc094

21. Eslamloo-Grami M., Munir Z.A. The mechanism of combustion synthesis of titanium carbonitride. *Journal of Materials Research*. 1994;9(2):431–435. https://doi.org/10.1557/JMR.1994.0431

22. Mukasyan A.S., Rogachev A.S. Combustion synthesis: Mechanically induced nanostructured materials. *Journal of Materials Science*. 2017;52:11826–11833. https://doi.org/10.1007/s10853-017-1075-9

23. Mukasyan A.S., Lin Y.C., Rogachev A.S., Moskovskikh D.O. Direct combustion synthesis of silicon carbide nanopowder from the elements. *Journal of the American Ceramic Society*. 2013;96(1):111–117. https://doi.org/10.1111/jace.12107

24. Buinevich V.S., Nepapushev A.A., Moskovskikh D.O., Trusov G.V., Kuskov K.V., Vadchenko S.G., Rogachev A.S., Mukasyan A.S. Fabrication of ultra-high-temperature nonstoichiometric hafnium carbonitride via combustion synthesis and spark plasma sintering. *Ceramics International*. 2020; 46(10):16068–16073. https://doi.org/10.1016/j.ceramint.2020.03.158

25. Khadyrova I., Suvorova V., Nepapushev A., Suvorov D., Kuskov K., Moskovskikh D. Hafnium-zirconium carbonitride (Hf,Zr)(C,N) by one step mechanically induced self-sustaining reaction: Powder synthesis and spark plasma

sintering. *Ceramics*. 2023;6(2):1129–1138. https://doi.org/10.3390/ceramics6020067

26. Suvorova V., Khadyrova I., Nepapushev A., Kuskov K., Suvorov D., Moskovskikh D. Fabrication and investigation of novel hafnium-zirconium carbonitride ultra-high temperature ceramics. *Ceramics International*. 2023;49(14):23809–23816. https://doi.org/10.1016/j.ceramint.2023.04.222

27. Merzhanov A.G., Rogachev A.S. Structural macrokinetics of SHS processes. *Pure and Applied Chemistry*. 1992; 64(7):941–953. https://doi.org/10.1351/pac199264070941

28. Deevi S.C. Structure of the combustion wave in the combustion synthesis of titanium carbides. *Journal of Materials Science*. 1991;26(10):2662–2670. https://doi.org/10.1007/BF00545552

29. Pikalova E.Y., Kalinina E.G., Pikalova N.S., Filonova E.A. High-entropy materials in SOFC technology: Theoretical foundations for their creation, features of synthesis, and recent achievements. *Materials*. 2022;15(24):8783. https://doi.org/10.3390/ma15248783

30. Golgovici F., Tudose A.E., Diniasi D., Nartit R., Fulger M., Demetrescu I. Aspects of applied chemistry related to future goals of safety and efficiency in materials development for nuclear energy. *Molecules*. 2023;28(2):874. https://doi.org/10.3390/molecules28020874

31. Han X.Q., Lin N., Li A.Q., Li J.Q., Wu Z.G., Wang Z.Y., He Y.H., Kang X.Y., Ma C. Microstructure and characterization of (Ti,V,Nb,Ta)(C,N) high-entropy ceramic. *Ceramics International*. 2021;47(24):35105–35110. https://doi.org/10.1016/j.ceramint.2021.09.053

32. Wen T., Ye B., Nguyen M.C., Ma M., Chu Y. Thermophysical and mechanical properties of novel high-entropy metal nitride-carbides. *Journal of the American Ceramic Society*. 2020;103(11):6475–6489. https://doi.org/10.1111/jace.17333

33. Li Z., Wang Z., Wu Z., Xu B., Zhao S., Zhang W., Lin N. Phase, microstructure and related mechanical properties of a series of (NbTaZr)C-based high entropy ceramics. *Ceramics International*. 2021;47(10):14341–14347. https://doi.org/10.1016/j.ceramint.2021.02.013

34. Ye B., Wen T., Nguyen M.C., Hao L., Wang C.Z., Chu Y. First-principles study, fabrication and characterization of $(Zr_{0.25}Nb_{0.25}Ti_{0.25}V_{0.25})C$ high-entropy ceramics. *Acta Materialia*. 2019;170:15–23. https://doi.org/10.1016/j.actamat.2019.03.021

35. Yan X., Constantin L., Lu Y., Silvain J.F., Nastasi M., Cui B. $(Hf_{0.2}Zr_{0.2}Ta_{0.2}Nb_{0.2}Ti_{0.2})C$ high-entropy ceramics with low thermal conductivity. *Journal of the American Ceramic Society*. 2018;101(10):4486–4491. https://doi.org/10.1111/jace.15779

Information about the Authors

Veronika S. Suvorova – Cand. Sci. (Eng.), Researcher at the Research Center of Engineering Ceramic Nanomaterials at the National University of Science and Technology "MISIS" (NUST MISIS)
ORCID: 0000-0002-0335-9153
E-mail: buynevich.vs@misis.ru

Andrey A. Nepapushev – Cand. Sci. (Eng.), Researcher at the Research Center of Engineering Ceramic Nanomaterials, NUST MISIS
ORCID: 0000-0001-9017-9937
E-mail: anepapushev@gmail.com

Dmitry S. Suvorov – Engineer at the Department of Functional Nanosystems and High Temperature Materials, NUST MISIS
ORCID: 0000-0002-0358-9987
E-mail: suvorov.ds@misis.ru

Kirill V. Kuskov – Leading Expert at the Research Center of Engineering Ceramic Nanomaterials, NUST MISIS
ORCID: 0000-0002-9387-0237
E-mail: kkuskov@misis.ru

Dmitry O. Moskovskikh – Cand. Sci. (Eng.), Director of the Research Center of Engineering Ceramic Nanomaterials, NUST MISIS
ORCID: 0000-0001-5168-4885
E-mail: mos@misis.ru

Сведения об авторах

Вероника Сергеевна Суворова – к.т.н., науч. сотрудник НИЦ «Конструкционные керамические наноматериалы» Национального исследовательского технологического университета «МИСИС» (НИТУ МИСИС)
ORCID: 0000-0002-0335-9153
E-mail: buynevich.vs@misis.ru

Андрей Александрович Непапушев – к.т.н., ст. науч. сотрудник НИЦ «Конструкционные керамические наноматериалы» НИТУ МИСИС
ORCID: 0000-0001-9017-9937
E-mail: anepapushev@gmail.com

Дмитрий Сергеевич Суворов – инженер кафедры функциональных наносистем и высокотемпературных материалов НИТУ МИСИС
ORCID: 0000-0002-0358-9987
E-mail: suvorov.ds@misis.ru

Кирилл Васильевич Кусков – вед. эксперт НИЦ «Конструкционные керамические наноматериалы» НИТУ МИСИС
ORCID: 0000-0002-9387-0237
E-mail: kkuskov@misis.ru

Дмитрий Олегович Московских – к.т.н., директор НИЦ «Конструкционные керамические наноматериалы» НИТУ МИСИС
ORCID: 0000-0001-5168-4885
E-mail: mos@misis.ru

Contribution of the Authors

V. S. Suvorova – determining the objective of the study, conducting experiments, writing the article.
A. A. Nepapushev – determining the objective of the study, writing the article.

Вклад авторов

В. С. Суворова – формулировка цели исследования, проведение экспериментов, написание статьи.
А. А. Непапушев – формулировка цели исследования, написание статьи.

D. S. Suvorov – conducting *X*-ray diffraction analysis, analyzing the particle size after mechanical activation and self-propagating high-temperature synthesis, participating in the discussion of the results.
K. V. Kuskov – studying the structure and elemental composition by SEM, participating in the discussion of the results.

D. O. Moskovskikh – studying the chemical composition of the samples, participating in the discussion of the results.

Д. С. Суворов – проведение рентгенофазового анализа, анализ размера частиц после механического активирования и самораспространяющегося высокотемпературного синтеза, участие в обсуждении результатов.
К. В. Кусков – исследование структуры и элементного состава образцов методом сканирующей электронной микроскопии, участие в обсуждении результатов.
Д. О. Московских – исследование химического состава образцов, участие в обсуждении результатов.

Received 28.09.2023
Revised 08.12.2023
Accepted 12.12.2023

Статья поступила 28.09.2023 г.
Доработана 08.12.2023 г.
Принята к публикации 12.12.2023 г.